VALES – III. The calibration between the dust continuum and interstellar gas content of star-forming galaxies

T. M. Hughes,[1]★ E. Ibar,[1] V. Villanueva,[1] M. Aravena,[2] M. Baes,[3] N. Bourne,[4] A. Cooray,[5] L. J. M. Davies,[6] S. Driver,[6,7] L. Dunne,[4,8] S. Dye,[9] S. Eales,[8] C. Furlanetto,[9,10] R. Herrera-Camus,[11] R. J. Ivison,[4,12] E. van Kampen,[12] M. A. Lara-López,[13] S. Maddox,[4,8] M. J. Michałowski,[4] I. Oteo,[4,12] D. Smith,[14] M. W. L. Smith,[8] E. Valiante,[8] P. van der Werf,[15] S. Viaene[3,14] and Y. Q. Xue[16]

[1]*Instituto de Física y Astronomía, Universidad de Valparaíso, Avda. Gran Bretaña 1111, Valparaíso, Chile*
[2]*Núcleo de Astronomía, Facultad de Ingeniería, Universidad Diego Portales, Av. Ejército 441, Santiago, Chile*
[3]*Sterrenkundig Observatorium, Universiteit Gent, Krijgslaan 281-S9, B-Gent 9000, Belgium*
[4]*Institute for Astronomy, University of Edinburgh, Royal Observatory, Edinburgh EH9 3HJ, UK*
[5]*Department of Physics and Astronomy, University of California, Irvine, CA 92697, USA*
[6]*International Centre for Radio Astronomy Research, University of Western Australia, Crawley, WA 6009, Australia*
[7]*School of Physics and Astronomy, University of St Andrews, North Haugh, St Andrews KY16 9SS, UK*
[8]*School of Physics and Astronomy, Cardiff University, The Parade, Cardiff CF24 3AA, UK*
[9]*School of Physics and Astronomy, University of Nottingham, University Park, Nottingham NG7 2RD, UK*
[10]*CAPES Foundation, Ministry of Education of Brazil, Brasília/DF 70040-020, Brazil*
[11]*Max-Planck-Institut für extraterrestrische Physik, Giessenbachstraße, D-85748 Garching, Germany*
[12]*European Southern Observatory, Karl-Schwarzschild-Strasse 2, D-85748 Garching, Germany*
[13]*Instituto de Astronomía, Universidad Nacional Autonoma de México, A.P. 70-264, 04510 México, D.F., México*
[14]*Centre for Astrophysics Research, University of Hertfordshire, Hatfield, Hertfordshire AL10 9AB, UK*
[15]*Leiden Observatory, Leiden University, PO Box 9513, NL-2300 RA Leiden, the Netherlands*
[16]*CAS Key Laboratory for Researches in Galaxies and Cosmology, Center for Astrophysics, Department of Astronomy, University of Science and Technology of China, Chinese Academy of Sciences, Hefei, Anhui 230026, China*

ABSTRACT

We present the calibration between the dust continuum luminosity and interstellar gas content obtained from the Valparaíso ALMA Line Emission Survey (VALES) sample of 67 main-sequence star-forming galaxies at $0.02 < z < 0.35$. We use CO(1–0) observations from the Atacama Large Millimetre/submillimetre Array to trace the molecular gas mass, M_{H_2}, and estimate the rest-frame monochromatic luminosity at 850 μm, $L_{\nu_{850}}$, by extrapolating the dust continuum from MAGPHYS modelling of the far-ultraviolet to submillimetre spectral energy distribution sampled by the Galaxy And Mass Assembly survey. Adopting $\alpha_{CO} = 6.5$ (K km s^{-1} pc^2)$^{-1}$, the average ratio of $L_{\nu_{850}}/M_{H_2} = (6.4 \pm 1.4) \times 10^{19}$ erg s^{-1} Hz^{-1} M$_{\odot}^{-1}$, in excellent agreement with literature values. We obtain a linear fit of $\log_{10}\left(M_{H_2}/M_{\odot}\right) = (0.92 \pm 0.02)\log_{10}(L_{\nu_{850}}/\text{erg s}^{-1}\text{ Hz}^{-1}) - (17.31 \pm 0.59)$. We provide relations between $L_{\nu_{850}}$, M_{H_2} and M_{ISM} when combining the VALES and literature samples, and adopting a Galactic α_{CO} value.

Key words: ISM: lines and bands – galaxies: ISM – submillimetre: galaxies.

1 INTRODUCTION

Disentangling the physical processes contributing to the decline in the overall cosmic star formation rate density (ρ_{SFR}) since the observed peak at $z \sim 2$ (e.g. Madau & Dickinson 2014) requires the

measurement of the gas content in the interstellar medium (ISM) of galaxies out to high redshift. The most reliable technique is to use the neutral hydrogen 21-cm line to trace the atomic gas phase and/or the CO molecule lines arising from rotational transitions to trace the molecular gas component (see e.g. Carilli & Walter 2013, and references therein). However, the linear relationship between the 21-cm line brightness and the column density of gas breaks for optically thick gas (Braun et al. 2009). Furthermore, the 'α_{CO}

★ E-mail: thomas.hughes@uv.cl

factor', the constant of proportionality between the mass of the molecular phase gas and the CO line emission, typically from the J = 1–0 or J = 2–1 line, is highly uncertain with a possible dependence on gas-phase metallicity (Wilson 1995; Israel 2005), galaxy kinematics, and excitation conditions (Solomon & Vanden Bout 2005). The standard CO/21-cm method may also overlook a significant fraction of lower column density molecular gas, which is not CO bright and so traced by neither line (Abdo et al. 2010; Planck Collaboration XIX 2011a). Technologically, it remains impossible to detect the H I line from galaxies at $z > 0.4$ with the current generation of facilities, and the detection of CO line emission typically requires long exposure times (several tens of hours) for normal, high redshift targets.

Faced with these observational difficulties, an alternative to the standard CO/21-cm methods for estimating the mass of the ISM in a galaxy at high redshift might be to use instead the continuum dust emission (see e.g. Hildebrand 1983; Dunne et al. 2000; Boselli, Lequeux & Gavazzi 2002). The *Herschel* Space Observatory (Pilbratt et al. 2010) with the Photodetector Array Camera and Spectrometer (PACS; Poglitsch et al. 2010) and the Spectral and Photometric Imaging REceiver (SPIRE; Griffin et al. 2010) were jointly capable of detecting the far-infrared (FIR) to submillimetre (submm) continuum emission originating from the dust component in six wavebands (70 to 500 µm) with significantly higher sensitivity and angular resolution than previous FIR/submm experiments, making it possible to derive a calibration between the dust emission and the ISM mass, M_{ISM} (Eales et al. 2012; Magdis et al. 2013), though the calibration is dependent on an accurate knowledge of the dust temperature.

Most recently, Scoville et al. (2016) used a calibration between the dust continuum at $\lambda = 850$ µm and the molecular gas content to infer the properties of higher redshift ($z \leq 6$) galaxies. The empirical calibration was obtained considering *Planck* observations of the Milky Way (Planck Collaboration XXI 2011b; Planck Collaboration XXV 2011c) and samples of low-redshift star-forming galaxies (Dale et al. 2005; Clements, Dunne & Eales 2010), ultra-luminous infrared galaxies (ULIRGs) and higher redshift ($z = 2$–3) submillimetre galaxies (SMGs) from the literature. Although they report that each method yields a similar rest-frame 850 µm luminosity per unit ISM mass, the calibration based on the sample of 70 star-forming galaxies, SMGs and ULIRGs, gave $L_{\nu_{850}}/M_{H_2} = (6.7 \pm 1.7) \times 10^{19}$ erg s^{-1} Hz^{-1} M$_\odot^{-1}$. By applying their calibration to ALMA observations of galaxies in three redshift bins up to $z = 4.4$, Scoville et al. conclude that starburst galaxies above the main sequence are largely the result of having greatly increased gas masses rather than an increased efficiency of converting gas to stars, with star-forming galaxies at $z > 1$ exhibiting ~2–5 times shorter gas depletion times than low-z galaxies. Whilst the application of this empirical calibration (see also Scoville et al. 2017) has clear advantages, being much faster (~20×) at estimating the ISM mass than molecular line observations and applicable to more readily obtainable continuum observations at higher redshift, the method assumes a solar metallicity and so may not apply to lower mass, metal-poor galaxies at higher redshifts. It is crucial to test the robustness of this calibration to ensure that any evolution with redshift is in fact physical.

In this Letter, we present the calibration between the dust continuum and molecular gas content derived from measurements of $L_{\nu_{850}}$, M_{H_2} and M_{ISM} for an expanded, homogeneous sample of 67 main-sequence star-forming galaxies at $0.02 < z < 0.35$ in the Valparaíso ALMA Line Emission Survey (VALES; Hughes et al. 2016; Villanueva et al. 2017), based on a combination of Band-3 CO(1–0) observations taken with the Atacama Large Millimetre/submillimetre Array (ALMA) and FUV-submm photometry from the GAMA survey (Driver et al. 2016; Wright et al. 2016). We adopt a Λ cold dark matter cosmology with $H_0 = 70$ km s^{-1} Mpc^{-1}, $\Omega_M = 0.27$ and $\Omega_\Lambda = 0.73$.

2 THE SAMPLE AND DATA

2.1 Sample selection

Our sample of galaxies was originally drawn from the *Herschel* Astrophysical Terahertz Large Area Survey (Eales et al. 2010; Bourne et al. 2016; Valiante et al. 2016), a *Herschel* programme capable of providing a sufficient number of far-IR bright galaxies over ~600 deg^2 with a wealth of high-quality ancillary data. From the three equatorial fields spanning ~160 deg^2 covered by *H*-ATLAS, galaxies were selected based on the following criteria: (1) a flux of $S_{160\,\mu m} > 150$ mJy; (2) no neighbours with $S_{160\,\mu m} > 160$ mJy; (3σ) within 2 arcmin from their centroids; (3) an unambiguous identification (RELIABILITY > 0.8; Bourne et al. 2016) in the Sloan Digital Sky Survey (SDSS DR7; Abazajian et al. 2009); (4) a Petrosian SDSS *r*-band radius <15 arcsec, i.e. smaller than the PACS spectroscopic field of view; (5) high-quality spectroscopic redshifts (ZQUAL > 3) from the Galaxy and Mass Assembly survey (GAMA; Liske et al. 2015); and (6) a redshift between 0.02 $< z < 0.35$ (median of 0.05), beyond which the CO(1–0) line is redshifted out of ALMA Band 3. After applying these criteria, 324 galaxies remain to comprise a statistically-significant sample spanning a wide range of optical morphological types and IR luminosities. Of these, 67 objects have follow-up ALMA CO(1–0) line observations as part of VALES, and GAMA FUV to FIR/submm photometry. These galaxies have stellar masses from 6 to 11× 10^{10} M$_\odot$, SFRs between 0.6 and 100 M$_\odot$ yr^{-1}, and metallicities of $8.7 < 12 + \log_{10}(O/H) < 9.2$ (see Villanueva et al. 2017).

2.2 ALMA CO(1–0) line observations

We exploit our VALES observations targeting the CO(1–0) line in Band 3 for 67 galaxies obtained during cycle-1 and cycle-2. Villanueva et al. (2017) present the observations, data reduction and a detailed characterization for the complete sample. All observations were reduced homogeneously within the Common Astronomy Software Applications[1] (CASA; McMullin et al. 2007) using a common pipeline, developed from standard pipelines, for calibration, concatenation and imaging, with standard bandpass, flux and phase calibrators. Velocity-integrated CO(1–0) flux densities, $S_{CO}\Delta v$, in units of Jy km s^{-1} were obtained by collapsing the cleaned, primary-beam-corrected data cubes between $\nu_{obs} - \nu_{FWHM}$ and $\nu_{obs} + \nu_{FWHM}$ and fitting these cubes with a Gaussian. We detect >73 per cent (49 of 67) of the targets with a >5σ peak line detection. We estimate upper limits as 5× the measured rms from the collapsed cubes set at 100 km s^{-1} spectral resolution and adopting $\nu_{FWHM} = 250$ km s^{-1}.

2.3 Gama multiwavelength photometry

All of our galaxies are present in the GAMA Panchromatic Data Release[2] (Driver et al. 2016) that provides imaging for over 230 deg^2 with photometry in 21 bands extending from the far-ultraviolet to

---

[1] http://casa.nrao.edu/index.shtml
[2] http://cutout.icrar.org/panchromaticDR.php

FIR from numerous facilities, currently including: GALaxy Evolution eXplorer (*GALEX*), Sloan Digital Sky Survey (SDSS), Visible and Infrared Telescope for Astronomy (VISTA), *Wide-field Infrared Survey Explorer* (*WISE*), and *Herschel*. These data are processed to a common astrometric solution from which homogeneous photometry is derived for ∼221 373 galaxies with $r < 19.8$ mag (see Wright et al. 2016), meaning the spectral energy distribution (SED) between 0.1 and 500 µm is available for each galaxy.

3 THE $L_{\nu_{850}}$–$M_{\rm ISM}$ CALIBRATION

3.1 Estimating the dust continuum luminosity

In the absence of measurements of the dust continuum at 850 µm, we adopt an estimate of the $L_{\nu_{850}}$ based on an extrapolation of the modelled SED. Our primary approach to estimate $L_{\nu_{850}}$ exploits the FUV–FIR/submm *H*-ATLAS/GAMA photometry available for all our galaxies modelled with the Bayesian SED fitting code, MAGPHYS (da Cunha, Charlot & Elbaz 2008). The code fits the panchromatic SED, giving special consideration to the dust–energy balance, from a library of optical and infrared SEDs derived from a generalized multicomponent model of a galaxy. The FIR/submm dust emission is modelled with five modified black bodies, of which two components have variable temperatures representing thermalized cold and warm dust and the other three components represent hot dust at 130, 250 and 850 K. Two geometries describe the dust distribution: Birth clouds of new stars contain only warm and hot circumstellar dust, whereas all five dust components may contribute to the dust in the diffuse ISM. As our focus is solely on estimating the rest-frame 850 µm continuum luminosity, we refer the reader to Driver et al. (in preparation) for details of the complete analysis of the MAGPHYS modelling of all the GAMA SEDs, yet note that Villanueva et al. (2017) demonstrate how the stellar masses, IR luminosities, $L_{\rm IR}$, and SFRs derived from MAGPHYS are consistent within the uncertainties to empirical estimates found in Ibar et al. (2015).

Using the best-fitting SEDs, we calculate the median model flux between 800 and 900 µm, $S_{\nu_{850}}$, and convert this flux – that ranges from 1 to 15 mJy – into a monochromatic rest-frame luminosity, $L_{\nu_{850}}$, in units of erg s^{-1} Hz^{-1}, via

$$L_{\nu_{850}} = 1.19 \times 10^{27} \, S_{\nu_{850}}({\rm Jy}) \, (1+z)^{-1} \, D_{\rm L}^2 \, K \; {\rm erg \; s^{-1} \; Hz^{-1}}, \qquad (1)$$

where $D_{\rm L}$ is the luminosity distance in Mpc and K is the K-correction given by equation (2) in Dunne et al. (2011), following their exact methodology.[3] In addition to FUV–FIR/submm SED modelling through MAGPHYS, we also examine the results of fitting the five *H*-ATLAS PACS/SPIRE photometric bands with a one-component modified blackbody as originally presented by Hildebrand (1983), assuming a power-law dust emissivity and either keeping the spectral index β as a free parameter or fixing the value at 1.8 (e.g. Galametz et al. 2012). In both cases, our best-fitting model fluxes are consistent and produce results that support the conclusions reached with the MAGPHYS SED fitting results. We then compute the uncertainty in $L_{\nu_{850}}$ from the standard deviation of the three luminosity values, we obtain from modelling the SEDs with MAGPHYS and the two fits with one-component modified black bodies adopting variable and fixed spectral indices.

---

[3] The mean scatter between $L_{\nu_{850}}$ calculated via the method presented in appendix A of Scoville et al. (2016) and that used here is ±5 per cent, and both methods yield similar scaling relations.

3.2 Measurement of the interstellar gas content

From our velocity-integrated CO(1–0) flux densities, $S_{\rm CO}\Delta{\rm v}$, in units of Jy km s^{-1}, we calculate the CO line luminosity, $L'_{\rm CO}$, in units of K km s^{-1} pc^2 following equation (3) of Solomon & Vanden Bout 2005, given as

$$L'_{\rm CO} = 3.25 \times 10^7 \, S_{\rm CO} \, \Delta{\rm v} \, \nu_{\rm obs}^{-2} \, D_{\rm L}^2 \, (1+z)^{-3}, \qquad (2)$$

where $\nu_{\rm obs}$ is the observed frequency of the emission line in GHz. The values for $L'_{\rm CO}$ are in the range of $(0.03 - 3.51) \times 10^{10}$ K km s^{-1} pc^2, with an average value of $(0.67 \pm 0.06) \times 10^{10}$ K km s^{-1} pc^2. The CO line luminosity can then be converted into the molecular gas mass (including the mass of He), $M_{\rm H_2}$, by assuming an $\alpha_{\rm CO}$ conversion factor (see equation 5 in Solomon & Vanden Bout 2005). Our VALES galaxies have high stellar masses ($\geq 10^{10}$ M$_\odot$), thus avoiding metal-poor systems in which the dust-to-gas abundance ratio is expected to decrease nor where significant molecular gas exists without CO emission (see e.g. Bolatto, Wolfire & Leroy 2013).

We first exclude from our analysis, the merger/interacting systems identified using a K-band-based morphological classification as outlined in Villanueva et al. (2017). To facilitate a direct comparison with the results of Scoville et al., we primarily adopt $\alpha_{\rm CO} = 6.5$ (K km s^{-1} pc^2)$^{-1}$ for the bulge- and disc-dominated galaxies with normal star formation. In our 43 normal galaxies with detected CO emission, we derive $M_{\rm H_2}$ values in the range of $\log M_{\rm H_2}/M_\odot = 9.35 - 11.12$ with an median of 10.46 ± 0.01. Finally, to estimate the atomic hydrogen content, $M_{\rm HI}$, we use the H ɪ–colour scaling relation given by equation (4) of Zhang et al. (2009) with the $g - r$ colour and i–band surface brightness available from the GAMA photometry. The H ɪ mass ranges between $\log M_{\rm HI}/M_\odot = 8.55 - 10.54$ with an average of 9.57 ± 0.03 and typical errors of ±30 per cent. We then calculate the ISM gas mass as $M_{\rm ISM} = M_{\rm HI} + M_{\rm H_2}$ using standard error propagation.

3.3 The $L_{\nu_{850}}/M_{\rm ISM}$ calibration

Bringing these measurements together, we now examine the calibrations between the dust continuum and gas content found for the galaxies in our VALES sample considering only those galaxies with CO line detections. The VALES sample exhibits a mean ratio $S_{\rm CO}\Delta{\rm v}/S_{\nu_{850}}$ of 1081 ± 265 km s^{-1}, corrresponding to a mean $L'_{\rm CO}$ to $L_{\nu_{850}}$ ratio of $(2.91 \pm 0.66) \times 10^{-21}$ in units of the luminosity ratio dimensions (see Fig. 1), which is in agreement with that found (3.02×10^{-21}) for the three galaxy samples analysed in Scoville et al. (2016). In particular, the VALES galaxies have properties more akin to the low-z normal star-forming galaxies and ULIRGs than the SMG sample. After converting the CO luminosity into molecular gas mass, we find average ratios of $S_{\nu_{850}}/M_{\rm H_2} = (6.9 \pm 5.6) \times 10^{-13}$ Jy M$_\odot^{-1}$ and $L_{\nu_{850}}/M_{\rm H_2} = (6.4 \pm 1.4) \times 10^{19}$ erg s^{-1} Hz^{-1} M$_\odot^{-1}$, also in excellent agreement with the mean values found by Scoville et al. (2016) and with near-matching scatter.

Although a constant ratio is appropriate to describe the average properties of the both the Scoville et al. and VALES samples across the luminosity range, there is a very minor trend that galaxies with $L_{\nu_{850}} > 10^{30}$ erg s^{-1} Hz^{-1} tend to lie on or above the average ratio (see Fig. 2). Galaxies with $L_{\nu_{850}}$ fainter than this luminosity have slightly lower ratios than the average. Our results suggest that adopting a constant $L_{\nu_{850}}/M_{\rm H_2}$ ratio to estimate the ISM mass would underestimate $M_{\rm H_2}$ in galaxies where $L_{\nu_{850}} > 10^{30}$ erg s^{-1} Hz^{-1} (and vice versa) and so a linear fit (in logarithmic space) may be more
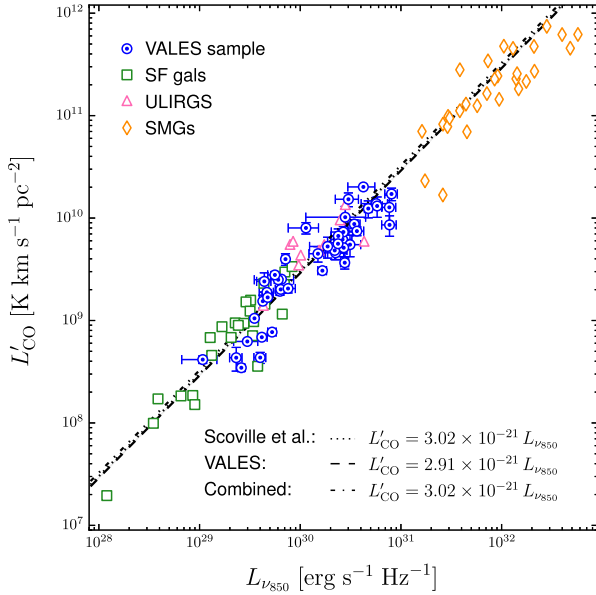
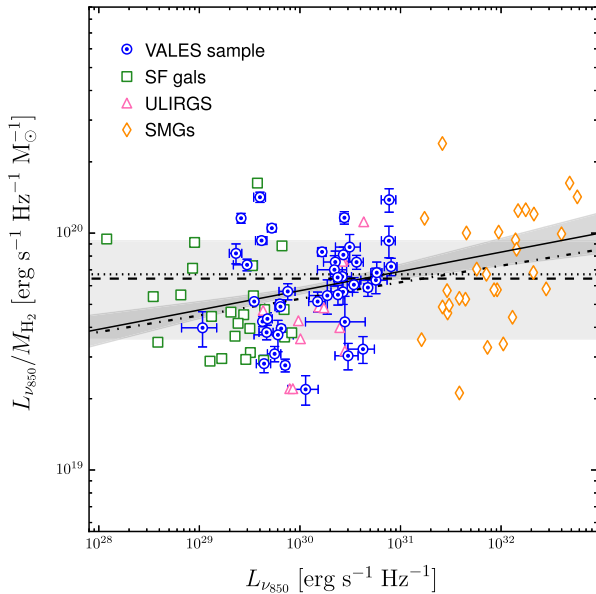**Figure 1.** The correlation between $L_{\nu_{850}}$ and L'_{CO} found for galaxies in our VALES sample observed with ALMA (Hughes et al. 2016; Villanueva et al. 2017). For galaxies with CO detections (blue circles), we show the average ratio (black dashed line) and compare to the mean value (black dotted line) found for the low-z samples of star-forming galaxies (SF; squares), ultra-luminous infrared galaxies (ULIRGs; triangles) and submillimetre galaxies (SMGs; diamonds) studied in Scoville et al. (2016). The average of these combined samples is superimposed (dashed–dotted line).

Figure 2. The ratio of $L_{\nu_{850}}$ to M_{H_2} found for galaxies in our VALES sample observed with ALMA (Hughes et al. 2016; Villanueva et al. 2017). From galaxies with CO detections (blue circles), we show the average ratio (black dashed line) with the $\pm 1\sigma$ range (light grey region) and the best linear fit (black solid line) with $\pm 1\sigma$ confidence limits (dark grey region). The low-z samples of SF galaxies (squares), ULIRGs (triangles) and SMGs (diamonds) are shown together with the mean value (black dotted line), taken from fig. 1 of Scoville et al. (2016).

Table 1. The best-fitting relations between the dust continuum luminosity at 850 μm (in units of erg s^{-1} Hz^{-1}) and various parameters considered in this work, expressed as $\log_{10} y = m \log_{10} L_{\nu_{850}} + c$, with the corresponding 1σ errors. We also state the scatter in dex (σ), Spearman (ρ_S) and Pearson (ρ_P) coefficients, where the values have probabilities P(ρ_P) and P(ρ_S) of >99.9 per cent that each of the two variables correlate for sample size $N = 43$ or 113. ^{a}Combined sample of 113 galaxies in VALES and Scoville et al. (2016).

y	m	c	σ	ρ_P	ρ_S
VALES sample only; $\alpha_{CO} \equiv 4.6$ (K km s^{-1} pc^2)$^{-1}$					
L'_{CO}	0.92 ± 0.02	-18.13 ± 0.59	0.12	0.94	0.92
$M_{H_2}/M_\odot$	0.92 ± 0.02	-17.46 ± 0.59	0.12	0.94	0.92
$M_{ISM}/M_\odot$	0.84 ± 0.02	-14.95 ± 0.54	0.11	0.94	0.92
Combined samples^a; $\alpha_{CO} \equiv 4.6$ (K km s^{-1} pc^2)$^{-1}$					
L'_{CO}	0.93 ± 0.01	-18.56 ± 0.05	0.12	0.98	0.98
$M_{H_2}/M_\odot$	0.93 ± 0.01	-17.90 ± 0.05	0.12	0.98	0.98
VALES sample only; $\alpha_{CO} \equiv 6.5$ (K km s^{-1} pc^2)$^{-1}$					
L'_{CO}	0.92 ± 0.02	-18.13 ± 0.59	0.12	0.94	0.92
$M_{H_2}/M_\odot$	0.92 ± 0.02	-17.31 ± 0.59	0.12	0.94	0.92
$M_{ISM}/M_\odot$	0.86 ± 0.02	-15.38 ± 0.55	0.12	0.94	0.92
Combined samples^a; $\alpha_{CO} \equiv 6.5$ (K km s^{-1} pc^2)$^{-1}$					
L'_{CO}	0.93 ± 0.01	-18.56 ± 0.05	0.12	0.98	0.98
$M_{H_2}/M_\odot$	0.93 ± 0.01	-17.74 ± 0.05	0.12	0.98	0.98

appropriate for the galaxies. For the VALES sample, we obtain

$$\log_{10} M_{H_2} = (0.92 \pm 0.02) \log_{10} L_{\nu_{850}} - (17.31 \pm 0.59), \quad (3)$$

$$\log_{10} M_{ISM} = (0.86 \pm 0.02) \log_{10} L_{\nu_{850}} - (15.38 \pm 0.55), \quad (4)$$

in which M and $L_{\nu_{850}}$ have units of $M_\odot$ and erg s^{-1} Hz^{-1}, respectively. This relation is valid between $1 \times 10^{29} < L_{\nu_{850}} < 2 \times 10^{31}$ erg s^{-1} Hz^{-1} for normal main-sequence star-forming galaxies and is based on the assumption that $\alpha_{CO} = 6.5$ (K km s^{-1} pc^2)$^{-1}$. Furthermore, we consider the calibrations we obtain from combining the 70 galaxies of Scoville et al. (2016) with the 43 CO-detected star-forming galaxies in our VALES sample. The $L_{\nu_{850}}$–M_{H_2} calibration for this combined sample of 113 objects is then

$$\log_{10} M_{H_2} = (0.93 \pm 0.01) \log_{10} L_{\nu_{850}} - (17.74 \pm 0.05) \quad (5)$$

with a scatter of ∼0.1 dex. However, the dominant error is on α_{CO} and is not included in our error calculations. We note that although Scoville et al. (2014) include the H I mass contribution to M_{ISM} (estimated as 50 per cent of the H$_2$ mass), Scoville et al. (2016) only consider the H$_2$ mass component, therefore we do not include a $L_{\nu_{850}}$–M_{ISM} calibration for the combined sample. We summarize these best-fitting relations and the corresponding correlation coefficients in Table 1, in which we also present the relations we obtain when adopting the Galactic value of $\alpha_{CO} = 4.6$ (K km s^{-1} pc^2)$^{-1}$ for our sample.

4 DISCUSSION

We have reported an updated calibration between the dust continuum and molecular gas content for an expanded sample of 67 main-sequence star-forming galaxies at $0.02 < z < 0.35$ drawn from the *H*-ATLAS, using gas mass measurements from ALMA Band-3 CO(1–0) observations and estimates of the monochromatic luminosity at 850 μm (rest frame), $L_{\nu_{850}}$, through an extrapolation of the dust continuum from MAGPHYS modelling of the FUV to

FIR/submm SED observed by the GAMA survey. Although we confirm an average $L_{\nu_{850}}/M_{H_2}$ ratio in close agreement with literature values (see Scoville et al. 2016, and references therein), the linear fit given by equation (4) alleviates the issue that the ISM mass may be overestimated for galaxies with lower continuum luminosities. Whilst we recommend using this best-fitting calibration rather than the constant calibration for estimating the gas content from dust continuum observations of main-sequence galaxies at high redshift, we stress that the largest uncertainty in this work remains in the α_{CO} factor.

Whichever value of α_{CO} we choose to adopt, using these Galactic-type values assumes that the CO emission comes from viriliazied molecular clouds bound by self-gravity. However, it remains possible that the CO line emission may actually trace material bound by the total potential of the galactic centre consisting of a mass of stars and dense gas clumps equal to the dynamical mass, M_{dyn}, and a diffuse interclump medium the CO emitting gas of mass M_{gas}. In this case, $M_{gas} = M_{dyn}(\alpha_{CO} L'_{CO})^2$ [see equation (6) in Solomon & Vanden Bout 2005], meaning the usual relation of α_{CO} will be changed if a fraction of the CO emission in our galaxies originates from an intercloud medium bound by the galaxy potential. Unfortunately, we currently have too few normal disc-dominated galaxies with spatially resolved CO emission (seven sources in total) to robustly identify whether such a change to the α_{CO} factor is warranted in our sample. We would also require more accurate estimates covering a greater dynamic range of metallicity in order to test the effect of the α_{CO} dependence on metallicity. In future VALES studies, we aim to use ALMA and MUSE to further investigate the robustness of the calibration between the dust continuum and molecular gas content with an α_{CO} constrained by 3D kinematical modelling for a larger sample of resolved galaxies.

REFERENCES

Abazajian K. N. et al., 2009, ApJS, 182, 543
Abdo A. A. et al., 2010, ApJ, 710, 133
Bolatto A. D., Wolfire M., Leroy A. K., 2013, ARA&A, 51, 207
Boselli A., Lequeux J., Gavazzi G., 2002, A&A, 384, 33
Bourne N. et al., 2016, MNRAS, 462, 1714
Braun R., Thilker D. A., Walterbos R. A. M., Corbelli E., 2009, ApJ, 695, 937
Carilli C. L., Walter F., 2013, ARA&A, 51, 105
Clements D. L., Dunne L., Eales S., 2010, MNRAS, 403, 274
da Cunha E., Charlot S., Elbaz D., 2008, MNRAS, 388, 1595
Dale D. A. et al., 2005, ApJ, 633, 857
Driver S. P. et al., 2016, MNRAS, 455, 3911
Dunne L., Eales S., Edmunds M., Ivison Rob., Alexander P., Clements D. L., 2000, MNRAS, 315, 115
Dunne L. et al., 2011, MNRAS, 417, 1510
Eales S. et al., 2010, PASP, 122, 499
Eales S. et al., 2012, ApJ, 761, 168
Galametz M. et al., 2012, MNRAS, 425, 763
Griffin M. J. et al., 2010, A&A, 518, L3
Hildebrand R. H., 1983, QJRAS, 24, 267
Hughes T. M. et al., 2016, A&A, preprint (arXiv:1611.05867)
Ibar E. et al., 2015, MNRAS, 449, 2498
Israel F. P., 2005, A&A, 438, 855
Liske J. et al., 2015, MNRAS, 452, 2087
Madau P., Dickinson M., 2014, ARA&A, 52, 415
Magdis G. E. et al., 2013, A&A, 558, A136
McMullin J. P., Waters B., Schiebel D., Young W., Golap K., 2007, in Shaw R. A., Hill F., Bell D. J., eds, ASP Conf. Ser. Vol. 376, Astronomical Data Analysis Software and Systems XVI. Astron. Soc. Pac., San Francisco, p. 127
Pilbratt G. L. et al., 2010, A&A, 518, L1
Planck Collaboration XIX, 2011a, A&A, 536, A19
Planck Collaboration XXI, 2011b, A&A, 536, A21
Planck Collaboration XXV, 2011c, A&A, 536, A25
Poglitsch A. et al., 2010, A&A, 518, L2
Scoville N. et al., 2014, ApJ, 783, 84
Scoville N. et al., 2016, ApJ, 820, 83
Scoville N. et al., 2017, preprint (arXiv:1702.04729)
Solomon P. M., Vanden Bout P. A., 2005, ARA&A, 43, 677
Valiante E. et al., 2016, MNRAS, 462, 3146
Villanueva V. et al., 2017, MNRAS, in press
Wilson C. D., 1995, ApJ, 448, L97
Wright A. H. et al., 2016, MNRAS, 460, 765
Zhang W., Li C., Kauffmann G., Zou H., Catinella B., Shen S., Guo Q., Chang R. et al., 2009, MNRAS, 397, 1243

This paper has been typeset from a TeX/LaTeX file prepared by the author.